ACS OMEGA

http://pubs.acs.org/journal/acsodf

Article

Kinetic Study on *Nannochloropsis Oculata*'s Lipid Extraction Using Supercritical CO_2 and *n*-Hexane for Biodiesel Production

Mohammadreza Askari, Ahmad Jafari, Feridun Esmaeilzadeh,* Mohammad Khorram, and Amir H. Mohammadi*

Cite This: *ACS Omega* 2022, 7, 23027−23040

Read Online

ACCESS | Metrics & More | Article Recommendations

ABSTRACT: Biodiesel as a renewable fuel has attracted increasing attention in recent years. Microalgae biomass is becoming an attractive raw material for producing biodiesel using supercritical CO_2 (SC-CO_2) as a safe and environmentally friendly technique with high efficiency for lipid extraction. In this study, the lipid of *Nannochloropsis oculata* was extracted under different conditions of SC-CO_2 to assess the kinetics of supercritical fluid extraction. The effective parameters on lipid extraction, including temperature, pressure, and the existence of *n*-hexane as a co-solvent, were investigated. The results show that an increase in temperature at low or high pressures causes the kinetic constant of lipid extraction to decrease or increase, respectively. Also, an increase in pressure causes the kinetic constant of lipid extraction to increase at low or high temperatures. The most yield and the most kinetic constant value during extraction with pure CO_2 are about 0.262 [g extracted lipid/g microalgal biomass] and 0.062 min^{-1}, respectively, at the highest pressure and temperature (i.e., 550 bar and 75 °C). Using SC-CO_2 laced with *n*-hexane increases both the final yield and the rate of lipid extraction. Also, it improves the quality of the biodiesel fuel through the extraction of unsaturated fatty acids with a concentration of almost two times more than saturated fatty acids. Additionally, results reveal that the effect of adding *n*-hexane to CO_2 in lipid extraction would be more efficient by increasing the temperature and lowering the pressure.

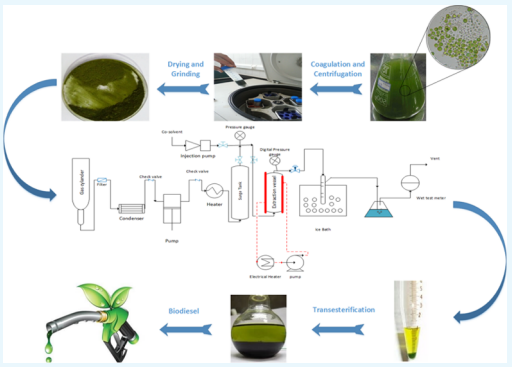

1. INTRODUCTION

The high consumption of fossil fuels not only causes a release of pollutants such as SO_X, NO_X, Hg, and ash in the atmosphere but also increases the greenhouse gas emission, which has intensive effects on the environment and human life, such as global warming[1] and increased fuel price due to the depletion of their resources.[2]

Finding a practical solution to these problems, which can lead to a sustainable energy source, is a complicated issue. It is related to the human life quality, the economic and industrial development of societies, and the profitability of super huge companies. It needs a worldwide district agreement such as the Kyoto protocol. Recently, so many ways have been developed to solve the problems mentioned above,[3] such as solar energy,[4] wind energy,[5] geothermal energy, biofuels,[6−8] and even converting biomass leftovers and by-products to biohydrogen[9] and hydrocarbon fuels.[10] Each one has gained different degrees of success in both study and application.

One of the most successful ideas is the gradual substitution of renewable energy sources for fossil fuels in transportation. Biofuels are the most possible substitutes for fossil fuels.[11] There are some reasons that make biofuels a decent alternative. First of all, biofuels can be applied without any change or with a bit of modification to the car's engine. Another reason is the issue of distribution. Biofuels can be distributed using the available distribution systems, unlike other options such as hydrogen.[12,13]

Biodiesel is a kind of biofuel that can be produced using either edible or non-edible oils. However, edible oils are not an economical feed for this process. One of the most appropriate feeds for biodiesel production is microalgal lipid.[5,14] In comparison to the other feedstocks, microalgae have their advantages. First of all, their growth rate is much higher than terrestrial crops. The other reasons are growing in the brine and on barren lands with various water qualities, requiring little care and maintenance, high concentration of intracellular lipid generation, and providing a new method for CO_2 recycling.[11,15−18] Some kinds of microalgae such as *Nannochloropsis oculata* (N. oculata) have very high biomass productivity

Received: July 28, 2021
Accepted: May 23, 2022
Published: June 24, 2022

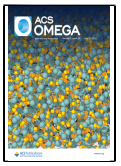

and also high lipid content,[12] which makes them suitable and economical for biodiesel production.

There are some conventional methods for microalgal lipid extraction using organic solvents such as *n*-hexane, ethanol, and chloroform. These methods have some problems such as toxicity, environmental problems, flammability, having low selectivity, and lipid degradation in high temperature and oxygen-rich conditions. Also, these methods need an additional separation process to separate lipid from the solvent.[19,20]

Supercritical fluid extraction (SFE) is an alternative method to conventional methods, which do not have these problems. Supercritical fluids have high solubility, low viscosity, high diffusivity, adjustable selectivity, and low surface tension.[21−23] Among supercritical fluids, supercritical CO_2 (SC-CO_2) was implicated in this study. In addition, SC-CO_2 omits the requirement for lipid−solvent separation. Also, it is an inflammable and cheaper solvent in comparison with other solvents.[24]

Among all the methods of extraction and various feedstocks, SFE was preferred as the extraction method, and *N. oculata* was used in this study. Although SFE is a green technology and has a high yield of lipid extraction, it needs a high-pressure operation and consequently a high capital investment and capital cost. For solving this problem, the effects of adding various amounts of *n*-hexane as a co-solvent to SC-CO_2 were investigated. Although there are previous and recent reports in the literature on both biodiesel production from microalgal lipid and SC-CO_2 extraction of microalgal lipid, the effect of using *n*-hexane as a co-solvent has not been extensively studied.[25−27] Using *n*-hexane as a co-solvent and studying its effects are the novelties of our research. For this purpose, the effects of different parameters including temperature (i.e., 35, 55, and 75 °C) and pressure (i.e., 150, 350, and 550 bars) were elucidated at the constant pure CO_2 flow rate of 200 mL/min, and then the effect of the co-solvent concentration (i.e., 1.5 and 3 wt %) was examined.

2. RESULTS AND DISCUSSION

In this study, four parameters, including extraction time, temperature, pressure, and mass percentage of the co-solvent, were investigated in 13 different tests. It should be mentioned that previous studies do not comprehensively consider the use of co-solvents and little work has been carried out on *n*-hexane as a co-solvent. The tested values are given in Table 1.

Table 1. Tested Values of the Examined Parameters

parameter	tested values
pressure, bar	150−350−550
temperature, °C	35−55−75
mass percentage of the co-solvent, wt %	0−1.5−3

All the results are given in Table 2.

It should be mentioned that changing a specific parameter may result in different results according to the other parameters. Therefore, to consider every aspect of any parameter, most of the results, in each set of conditions, are shown in several figures.

About 30% of the experiments were conducted twice to ensure the reproducibility of results. None of them showed more than a 5% deviation. Therefore, the margins of error bars in graphs are considered to be 5 percent.

As the effects of the two thermodynamic parameters of temperature and pressure are not independent of each other, in order to study one parameter, we should consider the effect of another parameter (i.e., variation of temperature has different effects on different pressures). Therefore, in order to study them, we changed both the temperature and the pressure simultaneously. Their effects are discussed separately in Sections 2.2 and 2.3.

First, the effects of temperature and pressure were examined using pure CO_2 at three different temperatures and pressures. It means there are nine different combinations of temperature and pressure. Then, to investigate the effect of the co-solvent, variations of temperature in the existence of the co-solvent, variations of pressure in the existence of the co-solvent, and variation of the co-solvent amount were studied in four different sets of conditions.

2.1. Pretreatment Effect. The pretreatment was conducted prior to extraction. Figures 1−3 show the scanning electron microscopy (SEM) images of the raw dry algae sample (before the pretreatment), milled algae (after the pretreatment), and the extracted algae (after the extraction by SC-CO_2), respectively. In raw dry microalgae, Figure 1, the cell membrane of the algae was completely intact and a high-density pack of the microalgae was observed. As shown in Figure 2, the cell wall after milling is wholly destroyed. As a result, the solvent can easily pass through the broken walls to extract lipid. Figure 3 shows the algal biomass after the extraction. An increase in porosity and further destruction of algal cells indicate an efficient lipid extraction from the prepared algal biomass using SC-CO_2. The obtained results are in complete agreement with the results reported by Özkal et al.[25]

2.2. Time and Temperature Effect. Temperature is one of the two crucial thermodynamic parameters (i.e., temperature and pressure), which can profoundly affect the extraction efficiency in SFE.[26] The duration of extraction in all the experiments was 5 h, and the CO_2 flow rate was fixed in all experiments at 200 mL/min. For each experiment, 20 g of the pretreated dry microalgae were loaded. Lipid extraction from the pretreated algal biomass was conducted at three different temperatures (i.e., 35, 55, and 75 °C). The variation of yield with time is shown in Figures 4−6 at different pressures. In all the figures, the extraction yield is shown by the points, and the lines are just to help the reader follow the experimental trends.

As can be seen, the extraction yield increases with increasing time and then levels off when it reaches equilibrium. In other words, the extraction rate is higher at the beginning of the extraction, and at the end of the experiment, the rate of lipid extraction becomes lower. The reason is that the rate of extraction at each time is directly proportional to the amount of unextracted lipid that remains any time in the biomass during the extraction.[27]

Increasing temperature causes two simultaneous effects. The first one is to reduce fluid density, which slows down the mass transfer, and the other is to increase the solubility of the solution, which increases the mass transfer rate.[2]

At a low pressure (i.e., 150 bar), which CO_2 density varies significantly with temperature ($\rho_{35\ °C}$ = 815.13 g/lit, $\rho_{55\ °C}$ = 654.5 g/lit, and $\rho_{75\ °C}$ = 463.55 g/lit), an increase in temperature causes a sharp decrease in the final yield of extraction (i.e., yield at 35 °C = 0.209, yield at 55 °C = 0.08, and yield at 75 °C = 0.006) and also a noticeable decrease in the kinetic constant of lipid extraction (i.e., $K_{at35\ °C}$ = 5.9 ×

https://doi.org/10.1021/acsomega.1c04029
ACS Omega 2022, 7, 23027−23040

Table 2. Experimental Data at a Given Time, Temperature, and Pressure

set 1: T = 35 °C, P = 150 bar (Figures 4, 7 and 11)											
t (min)	0	30	60	90	120	150	180	210	240	270	300
yield	0	0.04	0.074	0.102	0.126	0.145	0.162	0.176	0.188	0.197	0.206
set 2: T = 35 °C, P = 350 bar (Figures 5 and 7)											
t (min)	0	30	60	90	120	150	180	210	240	270	300
yield	0	0.137	0.2	0.23	0.243	0.25	0.252	0.254	0.254	0.255	0.255
set 3: T = 35 °C, P = 550 bar (Figures 6, 7 and 13)											
t (min)	0	30	60	90	120	150	180	210	240	270	300
yield	0	0.203	0.248	0.258	0.26	0.2606	0.2607	0.2608	0.2608	0.2608	0.2608
set 4: T = 55 °C, P = 150 bar (Figures 4 and 8)											
t (min)	0	30	60	90	120	150	180	210	240	270	300
yield	0	0.009	0.019	0.027	0.036	0.044	0.052	0.059	0.066	0.073	0.08
set 5: T = 55 °C, P = 350 bar (Figures 5 and 8)											
t (min)	0	30	60	90	120	150	180	210	240	270	300
yield	0	0.131	0.194	0.225	0.24	0.246	0.249	0.251	0.252	0.252	0.253
set 6: T = 55 °C, P = 550 bar (Figures 6 and 8)											
t (min)	0	30	60	90	120	150	180	210	240	270	300
yield	0	0.215	0.253	0.259	0.26	0.261	0.261	0.261	0.2612	0.2612	0.2612
set 7: T = 75 °C, P = 150 bar (Figures 4, 9 and 12)											
t (min)	0	30	60	90	120	150	180	210	240	270	300
yield	0	0.0006	0.001	0.002	0.0025	0.003	0.0037	0.004	0.005	0.0056	0.0062
set 8: T = 75 °C, P = 350 bar (Figures 5 and 9)											
t (min)	0	30	60	90	120	150	180	210	240	270	300
yield	0	0.11	0.171	0.206	0.225	0.236	0.242	0.245	0.247	0.248	0.249
set 9: T = 75 °C, P = 550 bar (Figures 6 and 9)											
t (min)	0	30	60	90	120	150	180	210	240	270	300
yield	0	0.218	0.255	0.26	0.261	0.262	0.262	0.262	0.262	0.262	0.262
set 10: T = 35 °C, P = 150 bar, 1.5 wt % *n*-hexane (Figure 11)											
t (min)	0	30	60	90	120	150	180	210	240	270	300
yield	0	0.091	0.148	0.185	0.209	0.224	0.233	0.239	0.243	0.245	0.247
set 11: T = 75 °C, P = 150 bar, 1.5 wt % *n*-hexane (Figure 12)											
t (min)	0	30	60	90	120	150	180	210	240	270	300
yield	0	0.0007	0.001	0.002	0.003	0.0036	0.004	0.005	0.006	0.0064	0.007
set 12: T = 35 °C, P = 550 bar, 1.5 wt % *n*-hexane (Figure 13)											
t (min)	0	30	60	90	120	150	180	210	240	270	300
yield	0	0.215	0.253	0.26	0.261	0.261	0.261	0.261	0.261	0.261	0.261
set 13: T = 35 °C, P = 150 bar, 3 wt % *n*-hexane (Figure 11)											
t (min)	0	30	60	90	120	150	180	210	240	270	300
yield	0	0.164	0.22	0.24	0.248	0.249	0.25	0.25	0.25	0.25	0.25

10^{-3} min^{-1}, $K_{at55\ °C} = 1.3 \times 10^{-3}$ min^{-1}, and $K_{at75\ °C} = 9 \times 10^{-5}$ min^{-1}), respectively.

However, at a high pressure (i.e., 550 bar), which CO_2 density does not change considerably with temperature ($\rho_{35\ °C}$ = 1018.5 g/lit, $\rho_{55\ °C}$ = 963.74 g/lit, and $\rho_{75\ °C}$ = 909.18 g/lit),[28] an increase in temperature does not remarkably affect the final yield (i.e., yield at 35 °C = 0.261, yield at 55 °C = 0.261, and yield at 75 °C = 0.262). However, increasing temperature causes the kinetic constant of lipid extraction from the pretreated algal biomass to increase ($K_{at35\ °C} = 4.78 \times 10^{-2}$ min^{-1}, $K_{at55\ °C} = 5.35 \times 10^{-2}$ min^{-1}, and $K_{at75\ °C} = 5.49 \times 10^{-2}$ min^{-1}), respectively.

This comparison clearly shows that at low and high pressures, density and solubility are the dominant parameters in the extraction, respectively. These results are consistent with those reported by Andrich et al.,[29] Yu et al.,[30] Rizvi et al.,[31] and, Favati et al.[32]

2.3. Pressure Effect. The effect of pressure on the SC-CO_2 extraction efficiency was evaluated by conducting the lipid extraction from the prepared algal biomass at three different pressures (i.e., 150, 350, and 550 bars). In all the experiments, the flow rate of carbon dioxide was kept constant at 200 mL/min. Also, the extraction time was considered to be about 5 h. Because the effect of pressure is temperature dependent, these pressures were examined at three different temperatures (i.e., 35, 55, and 75 °C).

Figures 7−9 clearly show that increasing the pressure at any temperature reduces the time required to reach equilibrium with a higher extraction rate. It is also seen that the highest extraction yield at 550 bar is about 0.262 [g extracted lipid/g microalgal biomass], which is 5.3% more than the highest yield at 150 bar (i.e., 0.209 g extracted lipid/g microalgal biomass).

This trend can be attributed to the increase in the dielectric constant or solvent polarity, which is directly dependent on the density. The dielectric constant or polarity of the supercritical solvent determines the intensity of the interaction between the solvent and organic molecules.[33] As shown in Table 3, increasing the density at a constant temperature with increasing pressure causes the dielectric constant to increase. Also, the kinetic constant of extraction (K) has an exponential ratio to increase in the fluid dielectric constant.

https://doi.org/10.1021/acsomega.1c04029
ACS Omega 2022, 7, 23027−23040

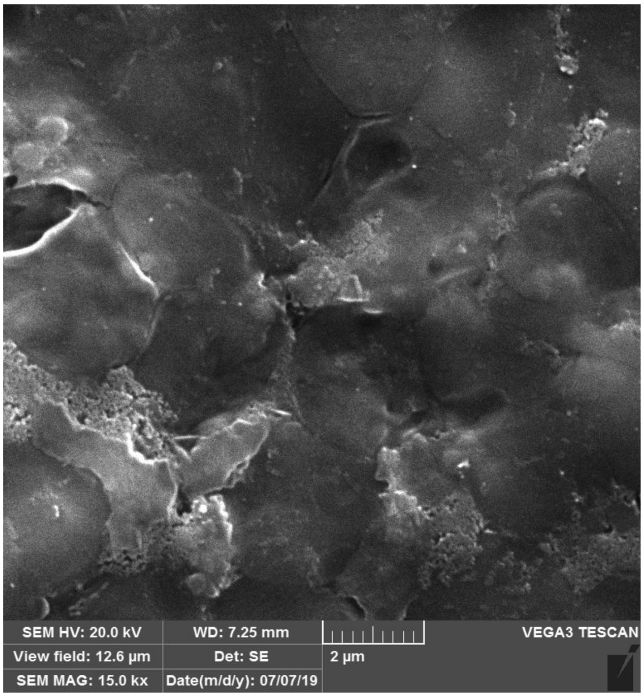

Figure 1. Raw dry algae sample (*N. oculata*, cultivation medium: F/2, illumination: 3000 Lux 12 h., coagulation agent: $FeCl_3$, dewatered in a benchtop centrifuge: 4000 rpm at 6 min).

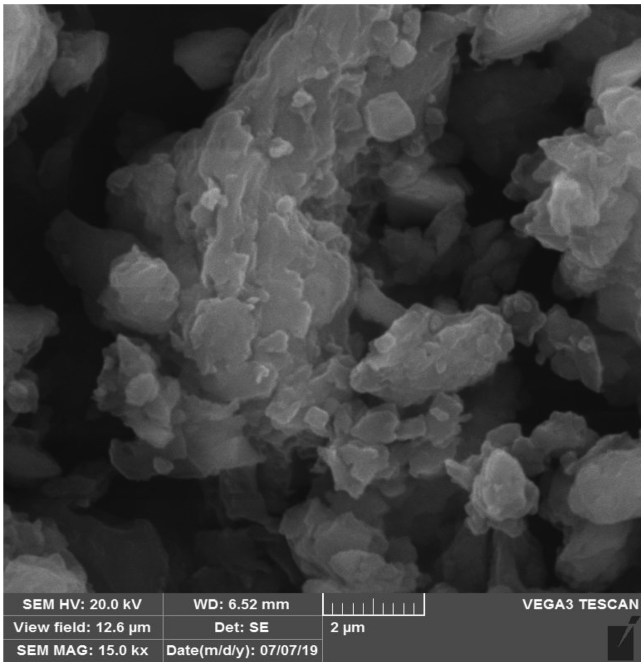

Figure 2. Milled biomass (dried in an oven: at 40 °C for 24 h, ground in a bead mill with different bead sizes at 5 h).

Additionally, obtained data were compared with those reported by Andrich et al.[29] shown in Figure 10. As can be seen, these results are approximately in line with those reported by Andrich et al.[29] at higher extraction times (i.e., higher than 150 min). However, a difference can be observed at lower extraction times and increases with decreasing extraction time from 120 to 30 min. The reason for this is that the kinetic constant of lipid extraction in this work (5.43×10^{-2} min^{-1}) is 162% higher than that reported by Andrich et al. (2.07×10^{-2} min^{-1}).[29] This increase is related to the technique used in the pretreatment of the biomass. In this work, the biomass was ground using a ball mill in 5 h. As shown in Figure 2, it caused the microalgae cell walls to destruct completely. As a result, lipid compounds in microalgae are exposed to SC-CO_2 for extraction at a higher rate, as stated by Teuling et al.[35]

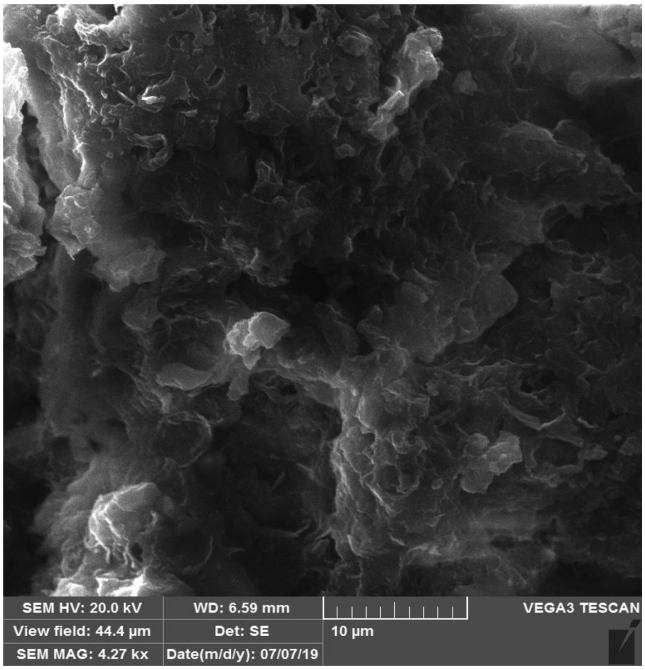

Figure 3. Algal biomass after SC-CO_2 extraction (extraction time: 5 h, temperature: 75 °C, pressure: 350 bar, co-solvent: 0 wt %).

Figure 10 shows that under the same conditions, the final extraction yield is the same. A very slight difference between them can be referred to differences in media and conditions of cultivation (i.e., this work's final yield is 0.2612 [g extracted lipid/g microalgal biomass] because Andrich et al.'s final yield is 0.2537 g extracted lipid/g microalgal biomass).

2.4. Co-solvent Effect. The SC-CO_2 laced with *n*-hexane in the range of 0−3 wt % was exploited to obtain the yield variations with time for the extraction of lipid from the algal biomass in the temperature and pressure ranges of 35−75 °C and 150−550 bar, respectively. The obtained results are shown in Figures 11−13.

As can be seen, adding *n*-hexane to CO_2 causes an increase in the final lipid extraction yield. This increase is due to the intermolecular interactions of *n*-hexane, CO_2, and lipids (i.e., solute−solute and solute−solvent interactions).

Figure 11 shows that using *n*-hexane as a co-solvent at the concentrations of 1.5 and 3 wt % at 35 °C and 150 bar causes the extraction yield to increase by about 20 and 21.4%, respectively, in comparison to SC-CO_2 alone (i.e., 0.206 [g extracted lipid/g microalgal biomass] for pure SC-CO_2, 0.247 and 0.25 [g extracted lipid/g microalgal biomass] for SC-CO_2 laced with 1.5 and 3 wt % *n*-hexane, respectively). Also, it shows that adding *n*-hexane as a co-solvent leads to an increase in the kinetic constant of extraction (i.e., $K_{\text{pure } co_2} = 5.9 \times 10^{-3}$ min^{-1}, $K_{1.5\%\ n\text{-hexane}} = 1.5 \times 10^{-2}$ min^{-1}, and $K_{3\%\ n\text{-hexane}} = 3.56 \times 10^{-2}$ min^{-1}). Additionally, it shows that adding 3% of *n*-hexane to low-pressure extraction (i.e., 35 °C and 150 bar)

https://doi.org/10.1021/acsomega.1c04029
ACS Omega 2022, 7, 23027−23040

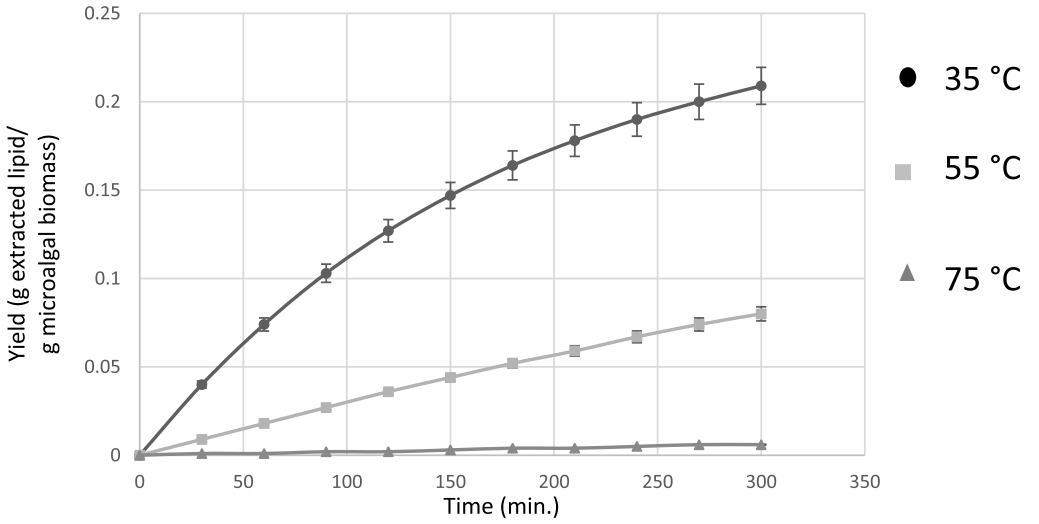

Figure 4. Variation in yield with time for the extraction of lipid from algal biomass at a pressure of 150 bar and different temperatures.

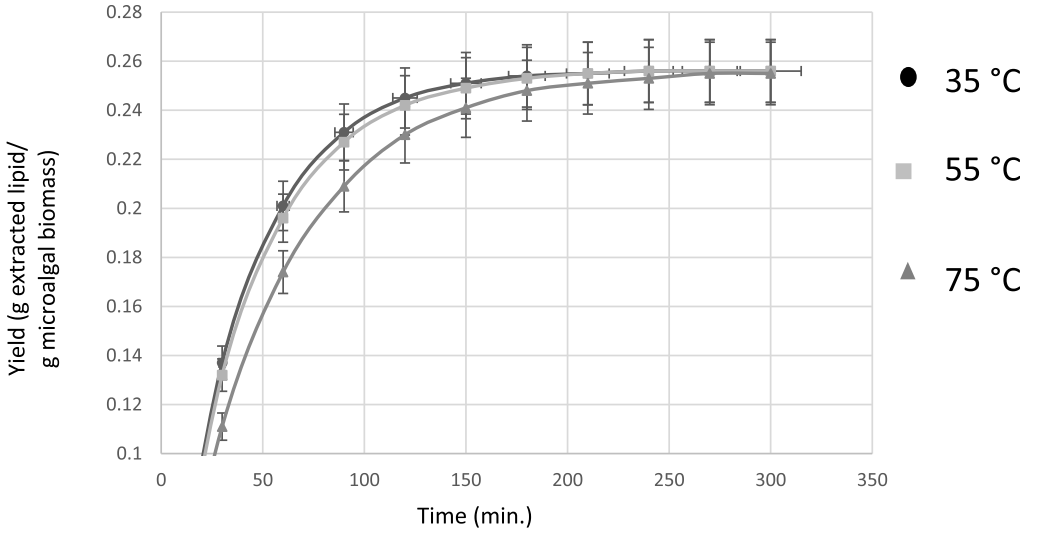

Figure 5. Variation in yield with time for the extraction of lipid from algal biomass at a pressure of 350 bar and different temperatures.

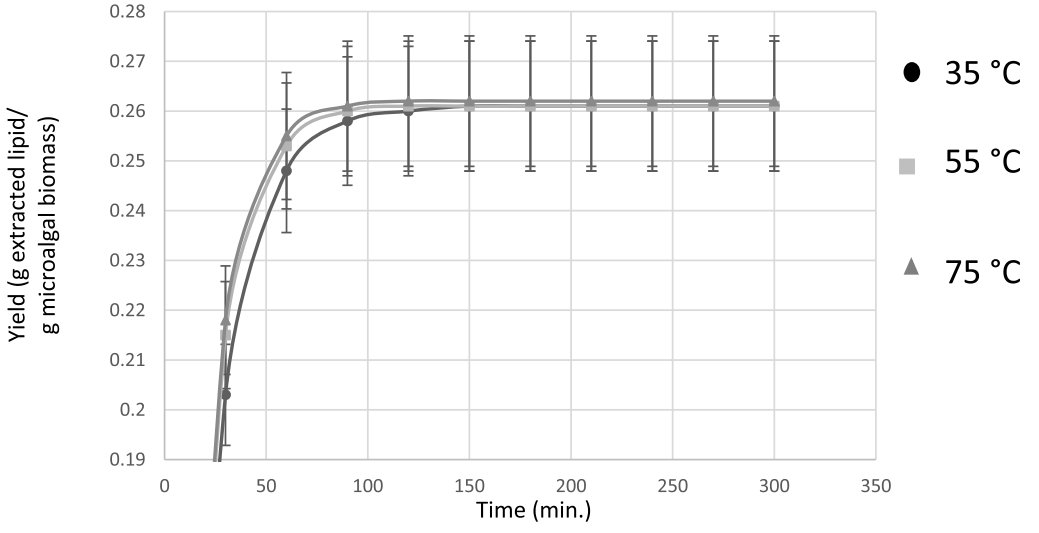

Figure 6. Variation in yield with time for the extraction of lipid from algal biomass at a pressure of 550 bar and different temperatures.

https://doi.org/10.1021/acsomega.1c04029
ACS Omega 2022, 7, 23027−23040

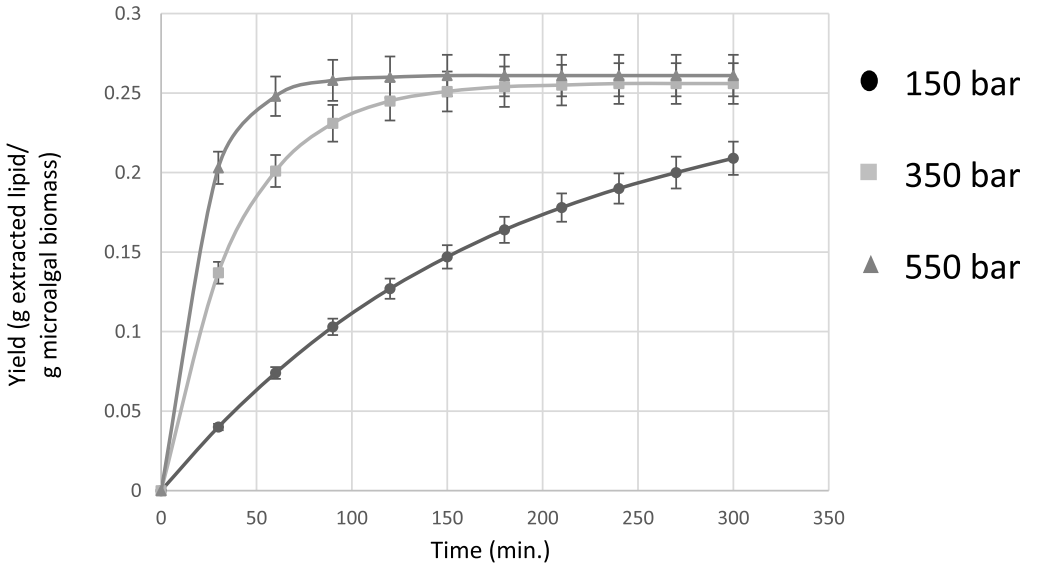

Figure 7. Variation in yield with time for the extraction of lipid from algal biomass at a temperature of 35 °C and different pressures.

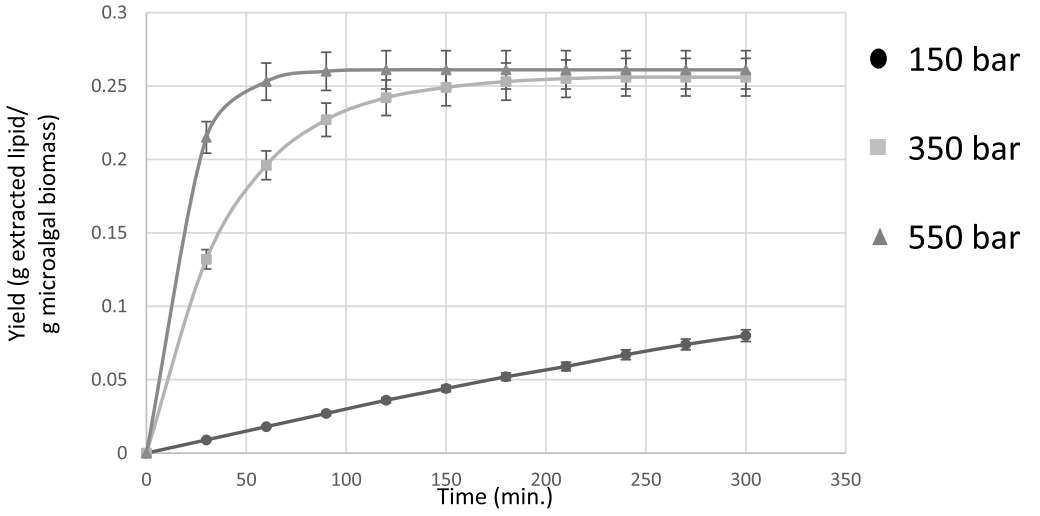

Figure 8. Variation in yield with time for the extraction of lipid from algal biomass at a temperature of 55 °C and different pressures.

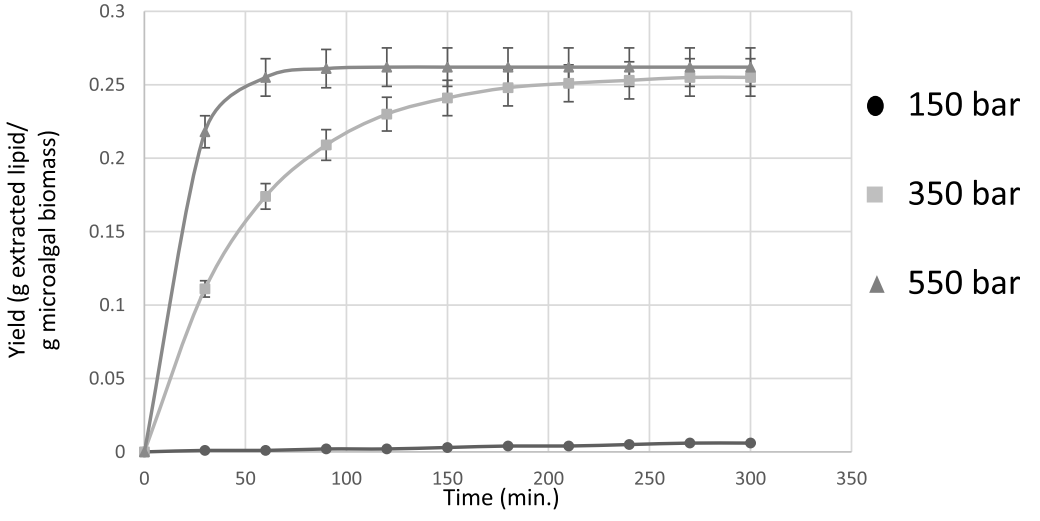

Figure 9. Variation in yield with time for the extraction of lipid from algal biomass at a temperature of 75 °C and different pressures.

https://doi.org/10.1021/acsomega.1c04029
ACS Omega 2022, 7, 23027−23040

Table 3. Variations of the Kinetic Constant of Extraction with the Dielectric Constant at 75 °C[33,34]

pressure (bar)	density (g/L)	SC-CO_2 dielectric constant	K (min^{-1})
150	467.0	1.300751	9×10^{-5}
350	808.4	1.488544	1.82×10^{-2}
550	910.2	1.562535	5.49×10^{-2}

makes its performance approach that of high-pressure extraction performance (i.e., 35 °C and 550 bar).

Figure 12 shows that using 1.5 wt % *n*-hexane with SC-CO_2 at 75 °C and 150 bar causes the extraction yield to increase to 0.007 [g extracted lipid/g microalgal biomass], which is too low (i.e., 0.0062 [g extracted lipid/g microalgal biomass] for pure SC-CO_2 and 0.007 [g extracted lipid/g microalgal biomass] for SC-CO_2 laced with 1.5 wt % *n*-hexane).

Figure 13 shows that using 1.5 wt % *n*-hexane with SC-CO_2 at 35 °C and 550 bar causes the extraction yield to not increase considerably compared to SC-CO_2 alone (i.e., 0.2608 [g extracted lipid/g microalgal biomass] for pure SC-CO_2 and 0.261 [g extracted lipid/g microalgal biomass] for SC-CO_2 laced with 1.5 wt % *n*-hexane).

Figure 11 also shows that SC-CO_2 laced with 3 wt % *n*-hexane at 35 °C and 150 bar causes the extraction yield to not increase considerably in comparison to SC-CO_2 alone (i.e., 0.2608 [g extracted lipid/g microalgal biomass] for pure SC-CO_2 and 0.261 [g extracted lipid/g microalgal biomass] for SC-CO_2 laced with 1.5 wt % *n*-hexane).

Generally, it can be concluded from Figures 11−13 that adding *n*-hexane to CO_2 at high pressures has no considerable effect on lipid extraction. On the other hand, at low pressures, adding *n*-hexane to CO_2 would increase the extraction yield and decrease the required extraction time. Therefore, it can be concluded that adding *n*-hexane and increasing pressure have similar effects, which can be related to the increasing solvent density. Also, it is evident that adding a small amount of the co-solvent can make a considerable economic saving in the capital investment, compared to a high-pressure operation and can omit the high operating cost of high-pressure supply.[36] Additionally, these results are consistent with those previously reported in the literature, as the report by Patil et al.[37]

2.5. Analysis of Fatty Acid Ethyl Esters with GC. The gas chromatography (GC) analysis was used to determine the composition of produced biodiesel. Table 4 shows the results of the GC analysis of SC-CO_2 extraction with and without *n*-hexane at 35 °C and 150 bar, separately.

As can be seen, the major components extracted by SC-CO_2 alone are C 14:0 (myristic acid) 39.46%, C 16:0 (palmitic acid) 18.51%, C 16:1 (palmitoleic acid) 18.50%, C 18:1 (oleic acid) 16.84%, and C 20:5 (eicosapantanoic acid) 3.74%. In addition, the major constituents of crude biodiesel extracted by SC-CO_2 laced with *n*-hexane are C 16:1 (palmitoleic acid) 28.71%, C 16:0 (palmitic acid) 27.34%, C 18:1 (oleic acid) 23.21%, C 20:5 (eicosapantanoic acid) 7.36%, C 14:0 (myristic acid) 4.69%, C 18:2 (linoleic acid) 3.35%, and C 20:4 (eicosatetraenoic acid) 2.46%.

Table 4 compares the quality of biodiesel extracted by SC-CO_2 alone and SC-CO_2 laced with *n*-hexane. It shows that SC-CO_2 extraction with *n*-hexane leads to the extraction of unsaturated fatty acids almost two times more than saturated fatty acids compared to SC-CO_2 alone, as mentioned in previous works.[38,39]

3. CONCLUSIONS

This study demonstrates that temperature has two different effects on the yield and the kinetic constant of extraction, depending on pressure. However, the pressure effect is independent of temperature. Also, the obtained results reveal that using *n*-hexane as a co-solvent has many advantages, such as increasing the yield at lower pressures and temperatures, increasing the lipid quality for biodiesel production, increasing the kinetic constant of extraction (k), and decreasing the required extraction time. All these useful effects are the results of the work's novelty, which is modifying the SFE by using *n*-hexane as a co-solvent.

Eventually, all of these effects must be seen as an economic saving. An economic study can be indicated as a possible drawback and limitation of study. Using *n*-hexane as a co-solvent can lead to a considerable decrease in the cost of biodiesel production. A comprehensive study on process economics and energy saving is suggested.

4. METHODOLOGY

4.1. Chemicals and Reagents. CO_2 gas with a purity of 99.9% was supplied by Aboughaddareh Company (Shiraz, Iran). *N*-hexane (≥99%) was provided by Sigma-Aldrich Pty., Ltd (Labco LLC, Dubai, UAE).

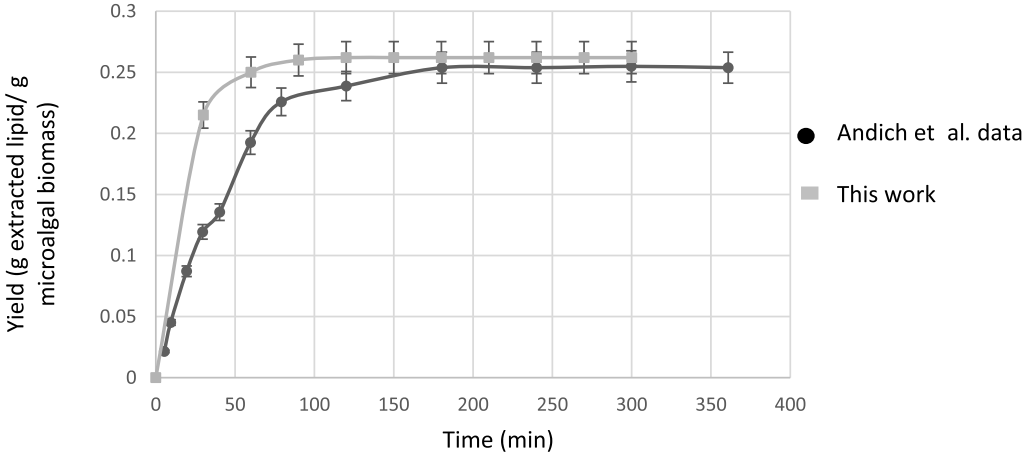

Figure 10. Comparison of this work's results (55 °C, 550 bar) to Andrich et al.'s data (55 °C, 550 bar).[29]

https://doi.org/10.1021/acsomega.1c04029
ACS Omega 2022, 7, 23027−23040

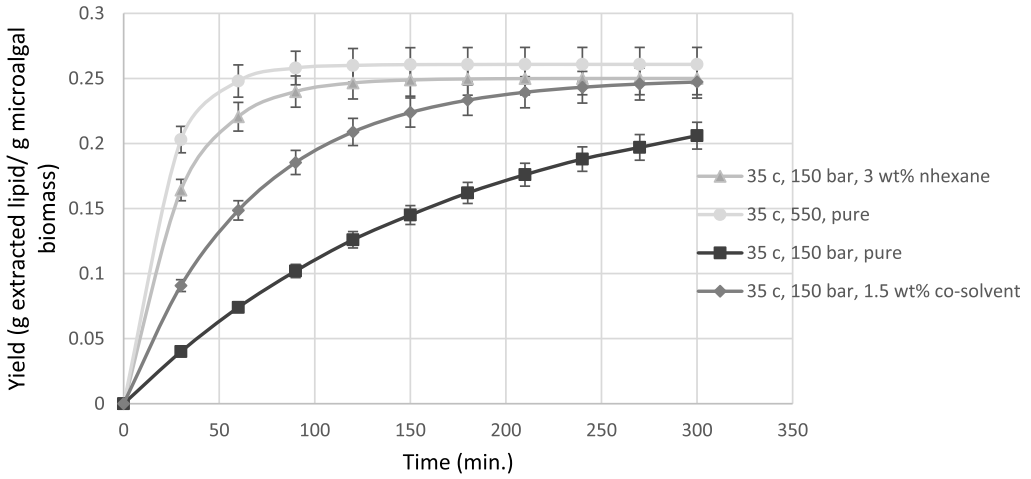

Figure 11. Variations in yield with time for the extraction of lipid from the algal biomass at 35 °C, different temperatures of 150 and 550 bar, with pure CO_2 and CO_2 laced with different percentages of *n*-hexane.

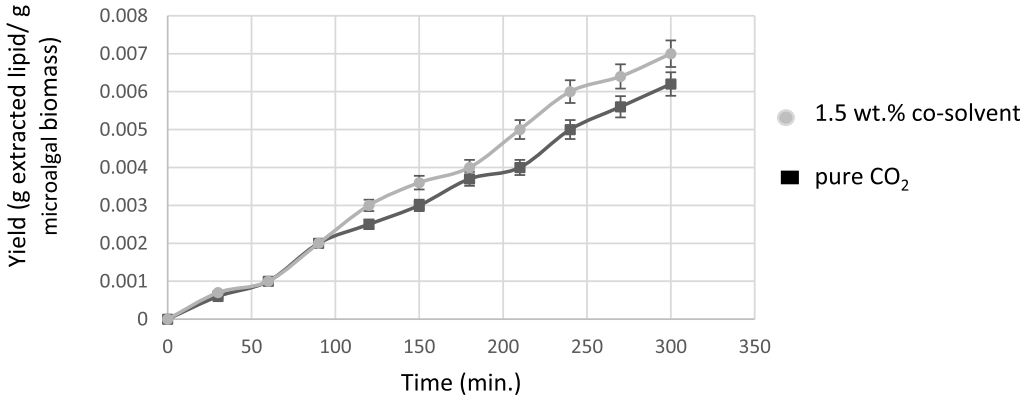

Figure 12. Variations in yield with time for the extraction of lipid from the algal biomass at 75 °C and 150 bar using SC-CO_2 laced with 1.5 wt % of *n*-hexane.

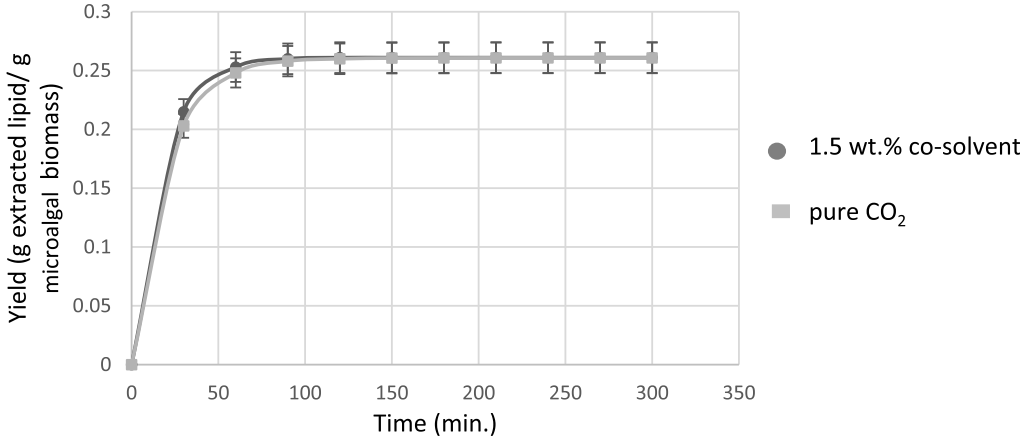

Figure 13. Variations in yield with time for the extraction of lipid from the algal biomass at 35 °C and 550 bar laced with different percentages of *n*-hexane.

4.2. Strain and Cultivation. The microalgae strain used in this study was *N. oculata,* which can be found naturally on the southern coastal beaches of Iran. It has a high lipid content and appropriate productivity.[11] A pure sample was provided by the Ecology Research Center of the Persian Gulf and Oman Sea (Bandar Abbas, Iran).

The elemental composition of algal biomass was determined by SEM equipped by energy dispersive X-ray spectroscopy (TESCAN-Vega3, Prague, Czech Republic). The major elements and their approximate composition in wt % were found to be carbon (61.55%), oxygen (20.79%), sodium (0.57%), magnesium (0.54%), silicium (0.59%), sulfur (0.87%), chlorine (11.88%), potassium (0.84%), and calcium (2.37%).

A set of 16 cylindrical bubble column bioreactors with an aspect ratio of 2 (with a height of 30 cm and a diameter of 15

https://doi.org/10.1021/acsomega.1c04029
ACS Omega 2022, 7, 23027−23040

Table 4. Fatty Acid Profiles of SC-CO_2 Extraction at 35 °C and 150 bar with and without *n*-Hexane

	extraction type	
component	pure SC-CO_2	SC-CO_2 laced with 3 wt % *n*-hexane
C 8:0	0.03	0.00
C 10:0	0.10	0.26
C 11:0	0.00	0.06
C 12:0	0.31	0.58
C 14:0	39.46	4.69
C 14:1	0.00	0.54
C 16:0	18.51	27.34
C 16:1	18.50	28.71
C 18:0	0.94	1.34
C 18:1	16.84	23.21
C 18:2	0.94	3.35
C 20:0	0.05	0.10
C 21:0	0.05	0.00
C 20:4	0.53	2.46
C 20:5	3.74	7.36
saturated fatty acids	59.45	34.37
unsaturated fatty acids	40.55	65.63
total	100	100

cm) was used for cultivation. The reactors were built from bottle-grade polyethylene terephthalate (Pars PET company, Tehran, Iran).

An F/2 medium was used for cultivation. Each bioreactor contained 15 L of microalgae culture and was kept at room temperature. Illumination was about 3000 lux, and it was in a periodic manner of 12 h of light and 12 h of darkness, along with the aeration using compressed air.

4.3. Harvesting. A 250 L of microalgal culture (with a concentration of 0.9 g dried microalgae/L) including 16 bioreactors were harvested simultaneously.

After growing for about 20 days, a coagulation agent ($FeCl_3$)[26] (Sigma−Aldrich, Labco LLC, Dubai, UAE) was added to the cultures, mixed, and given time to settle. The dilute part from the concentrated one was then separated. Next, the concentrated one was dewatered using a benchtop centrifuge (Eppendorf centrifuge 5810 R, Hamburg, Germany) at 4000 rpm for 6 min. Afterward, the algal paste was dissolved in the distilled water and centrifuged again to remove any residual salts.

4.4. Pretreatment. First, the microalgae were dried in an oven at 40 °C for 24 h. The dried microalgae were then ground using a bead mill with different bead sizes for 5 h. Then, the ground algal biomass was sieved using a standard sieve of 100 mesh. After the treatment, the prepared biomasses from all the bioreactors were blended to avoid any possible discrepancy in cultivation conditions in the following steps.

4.5. Apparatus and Procedures. A schematic diagram of the SFE apparatus is shown in Figure 14. A detailed description of the apparatus is reported in a previous work[40] with a bit of improvement. Here, it is explained briefly. CO_2 from a gas cylinder (1) was allowed to leave to a condenser (2), which turned it into liquefied carbon dioxide. Next, the liquefied carbon dioxide was entered into a high-pressure manual pump (Haskel pump, Burbank, USA) (3) to provide the desired pressure. The compressed liquid was then passed through a heater (4) to reach the appropriate temperature before entering the surge vessel (5) to dampen the pressure fluctuations generated by the operation of the hand pump. The pressurized CO_2 then entered an extraction vessel (150 mL, SS-316) (6). The extraction vessel was heated using a heating oil circulation jacket to set the extraction temperature constantly. A digital pressure indicator ranging up to 600 bar was used to monitor the pressure of the extraction vessel (WIKA, Taipei, Taiwan). The microalgae were placed in a layer of glass wool and loaded into a 100μ stainless steel mesh basket and then embedded in the extraction vessel. SC-CO_2

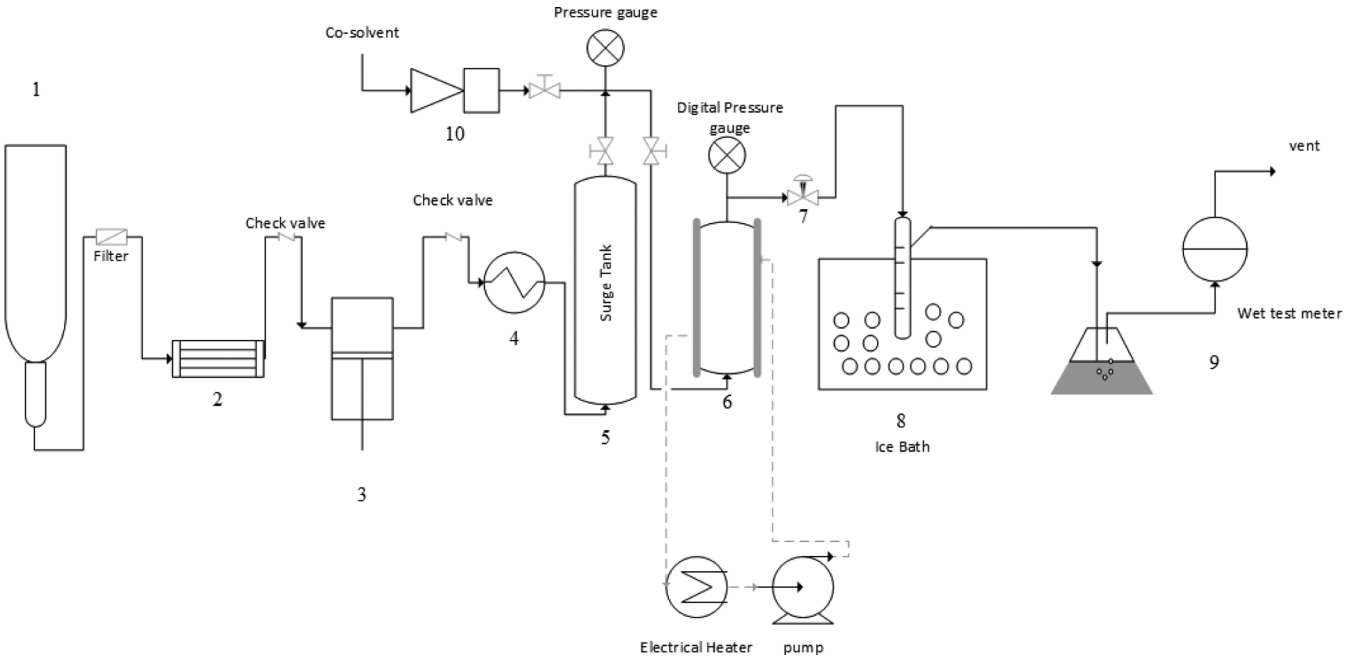

Figure 14. Schematic diagram of the SFE apparatus. (1) CO_2 gas cylinder; (2) condenser; (3) pump; (4) heater; (5) surge tank; (6) extraction vessel; (7) expansion valve; (8) ice bath; (9) wet test flowmeter; and (10) injection pump.

https://doi.org/10.1021/acsomega.1c04029
ACS Omega 2022, 7, 23027−23040

extracted lipids from the microalgae and then was directed to an expansion valve (7) to depressurize it to the ambient pressure. Afterward, the depressurized CO_2 was allowed to pass through a Y-type glass separator (8) embedded in an ice bath. Finally, the CO_2 was passed through a volumetric wet test flow meter (9) to measure the CO_2 flow rate, and the lipids accumulated in the glass separator were weighed using a digital balance (Sartorius, BA110s, Goettingen, Germany). Also, the apparatus was equipped with a co-solvent injection pump (Agilent HPLC, San Jose, USA) (10) to investigate the impact of co-solvent insolubility.

In this study, extraction was conducted in the pressure and temperature ranges of 150−550 bar and 35−75 °C, respectively. Also, the effect of *n*-hexane as a co-solvent was experimented with in two amounts of 1.5 and 3 weight percent of the co-solvent to CO_2 mass flow rate. To examine the effect of the co-solvent on the performance of lipid extraction, *n*-hexane as a co-solvent was injected into the solvent stream at various conditions.

It is worth mentioning that the pressure and temperature control were performed manually and automatically, respectively. Temperature control was performed using a proportional temperature control loop with the lowest span (i.e., 2 °C) in which below and above the set temperature, the controller adjusts the temperature by the turning electrical heater on or off. In order to control the pressure, after loading the prepared microalgae into the extraction vessel and setting the temperature, pressure was applied to the system using the manual pump while the outlet stream of the extractor was completely closed. After reaching the desired pressure, the outlet flow was adjusted by the expansion valve with the help of the wet test flow meter. Then, during the extraction, system pressure reduction was compensated by using the manual pump. Additionally, the fluctuation of the pressure generated using the pump was dampened by using the surge vessel.

At each extraction, a sample of 20 g of microalgae with 10 g of inert diatomaceous earth (d.e.) (particle size of 3−5 μm, biomass/d.e. = 2/1) was used. In all the experiments, the flow of CO_2 was constant and equal to 200 mL/min.

The extraction time was considered 5 h in all the experiments, and the lipid collector was replaced every 30 min. A pre-weighted collector was used each time.

A collector weight measurement was performed after disconnecting from the device, and the lipids were collected and kept in the refrigerator at −5 °C for the GC analysis. The results of the experiments were reported as the mass yield [g extracted lipid/g microalgal biomass], and the extraction trend diagram (yield versus time) was drawn and compared in all of the assessed conditions.

4.6. Extracted Lipid Analysis. Extraction performance was evaluated by two critical indicators in this study: lipid extraction yield and fatty acid methyl ester (FAME) composition at the end of each extraction.

The most important indicator of different parameters' (extraction time, temperature, pressure, and adding the co-solvent) effects on the extraction performance was lipid yield [g extracted lipid/g microalgal biomass]. The extraction lipid yield indicated quantitative efficiency. It was calculated by dividing the mass of extracted lipid by the mass of dry microalgal biomass in each extraction.

In order to distinguish FAME composition in the transesterified lipid, which indicated the quality of the extracted lipid, GC analysis was conducted.

The extracted lipid was transesterified to FAMEs using the method described by Halim et al.[2]

A volume of 0.4 μl of the transesterified lipid sample was injected into the GC instrument (Unicam GC, model 4600), which was equipped with a 30 m long capillary column (BPX70, 0.25 mm id, 0.22 μm film thickness) and a flame ionization detector. The injector and detector temperatures were set at 250 and 300 °C, respectively. The initial column temperature was 160 °C and was held for 5 min. It was then raised to 240 °C at a rate of 20 °C/min and was held for 9 min at that temperature (240 °C). The injector was set to split mode (split ratio: 1/100). Helium was used as the carrier gas. The FAMEs were identified according to the retention times of standard FAMEs, which were injected under the same operating conditions. Also, the concentration of FAMEs in the injected hexane solution was calculated by comparing their peak areas with those obtained from the standard peaks.

4.7. Extraction Kinetics. The proposed method used in this work to obtain the extraction kinetics is based on Fick's law of diffusion, which has been utilized by various researchers, such as Halim et al., Andrich et al., and Ozkal et al.[2,27,29]

Thus, the kinetic model was obtained as

$$\frac{dEO_t}{dt} = k(UO_t - UO_t^*) \quad (1)$$

where EO_t is the amount of extracted oil at time t per amount of microalgal biomass (g), UO_t represents the amount of unextracted oil (g) in 1 g of microalgal biomass, UO_t* stands for the amount of unextracted oil (g) when the equilibrium occurred in the extraction cell, t is the extraction time (min), and k represents the kinetic constant of extraction (min^{-1}).

Equation 1 is a simplified model of Fick's law in which the kinetic constant of extraction is assumed to be constant during the extraction.

In this model, $UO_t - UO_t$* is considered as the distance from the equilibrium. In other words, it represents the driving force of mass transfer.

Because fresh SC-CO_2 is continuously injected into the system, UO_t* can be considered to be zero; therefore

$$\frac{dEO_t}{dt} = k(UO_t) \quad (2)$$

Also

$$UO_t = UO_0 - EO_t \quad (3)$$

where UO_0 is the initial amount of lipid content in 1 g of microalgae. The phrase ($UO_0 - EO_t$) means the distance between the amount of lipid at the beginning of extraction and the amount of lipid extracted at time t; therefore

$$\frac{dEO_t}{dt} = k(UO_0 - EO_t) \quad (4)$$

By solving the abovementioned differential equation (eq 4) with the correct initial condition of ($EO_{t\ at\ t\ 0} = 0$), the following exponential equation is obtained

$$EO_t = UO_0(1 - e^{-kt}) \quad (5)$$

According to eq 5, the maximum extraction value is theoretically equivalent to UO_0. Therefore, it is assumed that the amount of UO_0 equals the maximum amount of lipid extracted (g) from 1 g of microalgae biomass in all the extractions. Hence

https://doi.org/10.1021/acsomega.1c04029
ACS Omega 2022, 7, 23027−23040

$$\ln\left(\frac{UO_0}{UO_0 - EO_t}\right) = kt \quad (6)$$

According to eq 6, the value of the lipid mass transfer coefficient, k, would be equal to the slope of the line passing through the points of the diagram of $\ln\left(\frac{UO_0}{UO_0 - EO_t}\right)$ versus t.

4.8. Statistical Analysis. *4.8.1. Analysis of Variance and Determination of the Significance Level.* A statistical test was performed using IBM SPSS Statistics 26 software to determine whether there was a significant difference between the three temperature groups, three pressure groups, and three amounts of co-solvent groups in the 10 time intervals in terms of the extraction yield.[41]

Table 5 shows the mean and standard deviation of the extraction yield in the three temperature and three pressure groups over 10 time intervals.

Table 5. Descriptive Statistics Table of the Extraction Yield in Three Temperature and Three Pressure Groups in 10 Time Intervals

temperature (°C)	pressure (bar)	average	standard deviation
35	150	0.13018	0.068821
	350	0.21291	0.079418
	550	0.23045	0.078359
55	150	0.04236	0.026785
	350	0.21109	0.079639
	550	0.23227	0.078246
75	150	0.00309	0.002071
	350	0.20245	0.080596
	550	0.23345	0.078528
Total	150	0.05855	0.067947
	350	0.20882	0.077488
	550	0.23206	0.075899

Table 6 shows the amount of the extraction yield studied in 10 time periods for three groups of temperature and three groups of pressure. According to the Fisher test, it is observed that the significance level (P-value) of the extraction yield in three groups of temperatures is less than 0.05, so there is a significant difference between them.

It has also been observed that the amount of the significance level (P-value) at the three pressure groups according to the Fisher test is less than 0.05, so there is a significant difference between the three pressure groups in terms of extraction yield.

After confirming the significance of the Fisher test in three temperature groups, the Duncan post-hoc test was used to examine which three temperature groups are significantly different in terms of extraction yield.

Table 7 shows that there is no significant difference in the amount of extraction yield in the two temperature groups of 75 and 55 (°C). Also, there is no significant difference in the amount of extraction yield in the two temperature groups of 55 and 35 (°C). However, the amount of extraction yield in the two temperature groups of 75 and 35 (°C) is significantly different. Figure 15 indicates significance pairwise comparison of the studied temperature groups based on extraction yield.

Table 7. Duncan Test in the Three Temperature Groups

		subset at a significance level of 0.05	
temperature (°C)	number	1	2
75	33	0.1463	
55	33	0.1619	0.1619
35	33		0.1911
P-Value		0.363	0.089

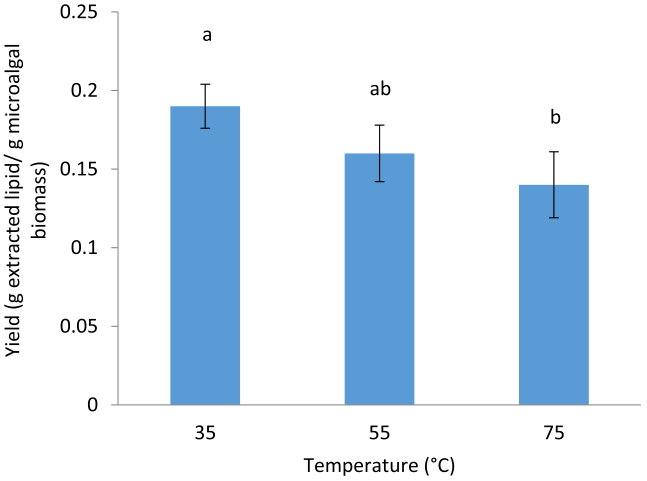

Figure 15. Significance pairwise comparison of the studied temperature groups based on extraction yield.

After confirming the significance of the Fisher test in three pressure groups, the Duncan post-hoc test was used to examine which three pressure groups are significantly different in terms of extraction yield.

Table 8 shows that there is no significant difference in the amount of extraction yield at the two pressure groups of 350 and 550 (bar). However, the amount of extraction yield for the group with a pressure of 150 bar is significantly different from the two other groups of pressure in pairs. Figure 16 shows the significance pairwise comparison of the studied pressure groups based on extraction yield.

Table 8. Duncan Test in the Three Pressure Groups

		subset at a significance level of 0.05	
pressure (bar)	number	1	2
150	33	0.0585	
350	33		0.2088
550	33		0.2320
P-Value		1.000	0.176

Table 6. Analysis of Variance of the Repeated Tests

source of changes	sum of squares	degrees of freedom	mean of squares	F-value	P-Value	effect rate	the amount of power
temperature	0.033	1	0.033	1.332	0.010	0.682	0.865
pressure	0.497	1	0.497	19.943	0.004	0.769	0.958
error	0.149	6	0.025				

https://doi.org/10.1021/acsomega.1c04029
ACS Omega 2022, 7, 23027−23040

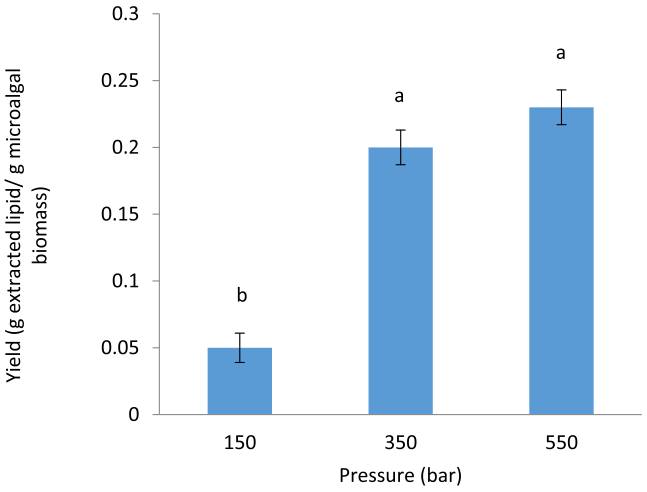

Figure 16. Significance pairwise comparison of the studied pressure groups based on extraction yield.

Table 9 indicates the mean and standard deviation of the amount of extraction yield in the three groups of 0, 1.5, and 3% of *n*-hexane as a co-solvent at 35 (°C) and 150 bar.

Table 9. Descriptive Statistics of Extraction Yield in Three Groups of 0, 1.5, and 3% of the Co-solvent at 35(°C) and 150 bar

co-solvent amount (wt %)	average	standard deviation
0%	0.13018	0.068821
1.5%	0.14973	0.075800
3%	0.15991	0.078443
total	0.14661	0.073181

In addition, one-way analysis of variance was conducted to investigate the significant difference in the amount of extraction yield between the three groups of 0, 1.5, and 3% of the co-solvent at 35 (°C) and 150 bar.

Table 10 shows the amount of extraction yield between the three groups with different percentages of the co-solvent studied by one-way analysis of variance.

Because the significance level below 0.05 is recognized as the significant level, and this parameter in this experiment was equal to 0.640 and is more than 0.05, there is no significant difference between the three studied groups.

4.8.2. Validity of the Calculated Kinetic Constants of Extractions (K). Equation 5 presents the yield of extraction for each set of parameters. To determine the relative accuracy of this equation, the following statistical parameters were calculated.[42]

Average percent error E_1

$$E_1 = \frac{1}{n}\sum_{i=1}^{n} r_i \tag{7}$$

Average absolute percent error E_2

$$E_2 = \frac{1}{n}\sum_{i=1}^{n} |r_i| \tag{8}$$

Standard percent deviation E_3

$$E_3 = \sqrt{\frac{1}{n-1} \times \sum_{i=1}^{n} (r_i - E_1)^2} \tag{9}$$

Root-mean square percent error E_4

$$E_4 = \sqrt{\frac{1}{n-1} \times \sum_{i=1}^{n} (r_i)^2} \tag{10}$$

where $r_i = [(\text{yield}_{\text{pred.}} - \text{yield}_{\text{expe.}})/\text{yield}_{\text{expe.}}] \times 100$ and n is the number of experimental data.

The comparison of these errors in the sets (1, 4, and 7), (2, 5, and 8), and (3, 6, and 9) in Table 11 shows that the lower the temperature and the higher the pressure, the better the fitted diagram fits the laboratory data. In other words, the lower the temperature and the higher the pressure, the more accurate and valid the amount of K would be obtained.

Table 11. E_1, E_2, E_3, and E_4 for Every Set of Conditions, which Is Described in Table 2

set	E_1 (%)	E_2 (%)	E_3 (%)	E_4 (%)
1	−42.85	42.85	22.36	50.40
2	−8.55	8.55	14.79	17.32
3	−3.13	3.13	7.49	8.18
4	−81.20	81.20	9.57	86.13
5	−10.11	10.11	16.21	19.40
6	−2.51	2.51	6.30	6.84
7	−98.53	98.53	0.81	103.86
8	−13.71	13.71	18.77	23.69
9	−2.39	2.39	6.04	6.54
10	−17.40	17.40	20.61	27.59
11	−98.37	98.37	0.89	103.69
12	−1.88	1.88	4.95	5.33
13	−5.24	5.24	10.88	12.20

AUTHOR INFORMATION

Corresponding Authors

Feridun Esmaeilzadeh − *Department of Chemical Engineering, School of Chemical and Petroleum Engineering, Shiraz University, Shiraz 7193616511, Iran*; Email: esmaeil@shirazu.ac.ir

Amir H. Mohammadi − *Discipline of Chemical Engineering, School of Engineering, University of KwaZulu-Natal, Durban 4041, South Africa*; orcid.org/0000-0002-2947-1135; Email: amir_h_mohammadi@yahoo.com

Table 10. One-Way Analysis of Variance of Extraction Yield in Three Groups of 0, 1.5, and 3% of the Co-solvent at 35(°C) and 150 bar

statistic indices	source of changes	degrees of freedom	sum of squares	mean of squares	*F*-value	*P*-Value
extraction yield between the three groups	group	2	0.005	0.003	0.453	0.640
	experiment error	30	0.166	0.006		
	coefficient of variation		35.0			

https://doi.org/10.1021/acsomega.1c04029
ACS Omega 2022, 7, 23027−23040

Authors

Mohammadreza Askari − *Department of Chemical Engineering, School of Chemical and Petroleum Engineering, Shiraz University, Shiraz 7193616511, Iran*

Ahmad Jafari − *Department of Chemical Engineering, School of Chemical and Petroleum Engineering, Shiraz University, Shiraz 7193616511, Iran*

Mohammad Khorram − *Department of Chemical Engineering, School of Chemical and Petroleum Engineering, Shiraz University, Shiraz 7193616511, Iran;* orcid.org/0000-0003-1542-2284

Complete contact information is available at: https://pubs.acs.org/10.1021/acsomega.1c04029

Notes

The authors declare no competing financial interest.

■ ACKNOWLEDGMENTS

The authors are grateful to the Shiraz University for financially supporting this study.

■ REFERENCES

(1) Palacios, A.; Barreneche, C.; Navarro, M.; Ding, Y. Thermal energy storage technologies for concentrated solar power−A review from a materials perspective. *Renew. Energy* **2020**, *156*, 1244.

(2) Halim, R.; Gladman, B.; Danquah, M. K.; Webley, P. A. Oil extraction from microalgae for biodiesel production. *Bioresour. Technol.* **2011**, *102*, 178−185.

(3) Kumar, S.; Jain, S.; Kumar, H. Experimental Study on Biodiesel Production Parameter Optimization of Jatropha−Algae Oil Mixtures and Performance and Emission Analysis of a Diesel Engine Coupled with a Generator Fueled with Diesel/Biodiesel Blends. *ACS Omega* **2020**, *5*, 17033−17041.

(4) Leirpoll, M. E.; Næss, J. S.; Cavalett, O.; Dorber, M.; Hu, X.; Cherubini, F. Optimal combination of bioenergy and solar photovoltaic for renewable energy production on abandoned cropland. *Renew. Energy* **2021**, *168*, 45.

(5) Willis, D. J.; Niezrecki, C.; Kuchma, D.; Hines, E.; Arwade, S. R.; Barthelmie, R. J.; DiPaola, M.; Drane, P. J.; Hansen, C. J.; Inalpolat, M.; Mack, J. H.; Myers, A. T.; Rotea, M. Wind energy research: State-of-the-art and future research directions. *Renew. Energy* **2018**, *125*, 133−154.

(6) Cancela, A.; Pérez, L.; Febrero, A.; Sánchez, A.; Salgueiro, J. L.; Ortiz, L. Exploitation of Nannochloropsis gaditana biomass for biodiesel and pellet production. *Renew. Energy* **2019**, *133*, 725−730.

(7) Dewulf, J.; Van Langenhove, H., *Renewables-Based Technology: Sustainability Assessment*; John Wiley & Sons, 2006.

(8) Gilbert, R.; Perl, A.; Banister, D. *Transport Revolutions: Moving People and Freight without Oil*; Earthscan, 2007.

(9) Nobre, B. P.; Villalobos, F.; Barragán, B. E.; Oliveira, A. C.; Batista, A. P.; Marques, P. A. S. S.; Mendes, R. L.; Sovová, H.; Palavra, A. F.; Gouveia, L. A biorefinery from Nannochloropsis sp. microalga−extraction of oils and pigments. Production of biohydrogen from the leftover biomass. *Bioresour. Technol.* **2013**, *135*, 128−136.

(10) Moula, M. M. E.; Nyári, J.; Bartel, A. Public acceptance of biofuels in the transport sector in Finland. *Int. J. Sustainable Built Environ.* **2017**, *6*, 434.

(11) Mata, T. M.; Martins, A. A.; Caetano, N. S. Microalgae for biodiesel production and other applications: a review. *Renew. Sustain. Energy Rev.* **2010**, *14*, 217−232.

(12) Hu, Q.; Sommerfeld, M.; Jarvis, E.; Ghirardi, M.; Posewitz, M.; Seibert, M.; Darzins, A. Microalgal triacylglycerols as feedstocks for biofuel production: perspectives and advances. *Plant J.* **2008**, *54*, 621−639.

(13) Shirneshan, A. R.; Almassi, M.; Ghobadian, B.; Najafi, G. Investigating the effects of biodiesel from waste cooking oil and engine operating conditions on the diesel engine performance by response surface methodology. *J. Sci. Technol.* **2014**, *38*, 289.

(14) Chisti, Y. Biodiesel from microalgae. *Biotechnol. Adv.* **2007**, *25*, 294−306.

(15) Azócar, L.; Heipieper, H. J.; Navia, R. Biotechnological processes for biodiesel production using alternative oils. *Appl. Microbiol. Biotechnol.* **2010**, *88*, 621−636.

(16) Huang, B.; Ban, X.; He, J.; Zeng, H.; Zhang, P.; Wang, Y. Hepatoprotective and antioxidant effects of the methanolic extract from Halenia elliptica. *J. Ethnopharmacol.* **2010**, *131*, 276−281.

(17) Doe, U. *National Algal Biofuels Technology Roadmap*; US Department of Energy, Office of Energy Efficiency and Renewable Energy, Biomass Program 2010.

(18) Wijffels, R. H.; Barbosa, M. J. An outlook on microalgal biofuels. *Science* **2010**, *329*, 796−799.

(19) Xu, H.; Miao, X.; Wu, Q. High quality biodiesel production from a microalga Chlorella protothecoides by heterotrophic growth in fermenters. *J. Biotechnol.* **2006**, *126*, 499−507.

(20) Herrero, M.; Vicente, M. J.; Cifuentes, A.; Ibáñez, E. Characterization by high-performance liquid chromatography/electrospray ionization quadrupole time-of-flight mass spectrometry of the lipid fraction of Spirulina platensis pressurized ethanol extract. *Rapid Commun. Mass Spectrom.* **2007**, *21*, 1729−1738.

(21) Sun, M.; Temelli, F. Supercritical carbon dioxide extraction of carotenoids from carrot using canola oil as a continuous co-solvent. *J. Supercrit. Fluids* **2006**, *37*, 397−408.

(22) Cheung, P. C. K.; Leung, A. Y. H.; Ang, P. O. Comparison of supercritical carbon dioxide and soxhlet extraction of lipids from a brown seaweed, Sargassum hemiphyllum (Turn.) C. Ag. *J. Agric. Food Chem.* **1998**, *46*, 4228−4232.

(23) Boocock, D. G. B.; Konar, S. K.; Mao, V.; Sidi, H. Fast one-phase oil-rich processes for the preparation of vegetable oil methyl esters. *Biomass Bioenergy* **1996**, *11*, 43−50.

(24) Ghoreishi, S. M.; Sharifi, S. Modeling of supercritical extraction of mannitol from plane tree leaf. *J. Pharm. Biomed. Anal.* **2001**, *24*, 1037−1048.

(25) Özkal, S. G.; Yener, M.; Bayındırlı, L. Mass transfer modeling of apricot kernel oil extraction with supercritical carbon dioxide. *J. Supercrit. Fluids* **2005**, *35*, 119−127.

(26) Halim, R.; Danquah, M. K.; Webley, P. A. Extraction of oil from microalgae for biodiesel production: A review. *Biotechnol. Adv.* **2012**, *30*, 709−732.

(27) Özkal, S. G.; Salgın, U.; Yener, M. E. Supercritical carbon dioxide extraction of hazelnut oil. *J. Food Eng.* **2005**, *69*, 217−223.

(28) Kennedy, G. C. Pressure-volume-temperature relations in CO2 at elevated temperatures and pressures. *Am. J. Sci.* **1954**, *252*, 225−241.

(29) Andrich, G.; Nesti, U.; Venturi, F.; Zinnai, A.; Fiorentini, R. Supercritical fluid extraction of bioactive lipids from the microalga Nannochloropsis sp. *Eur. J. Lipid Sci. Technol.* **2005**, *107*, 381−386.

(30) Yu, Z.-R.; Rizvi, S. S. H.; Zollweg, J. A. Phase equilibria of oleic acid, methyl oleate, and anhydrous milk fat in supercritical carbon dioxide. *J. Supercrit. Fluids* **1992**, *5*, 114−122.

(31) Rizvi, S. S. H.; Benado, A. L.; Zollweg, J. A.; Daniels, J. Supercritical fluid extraction: fundamental principles and modeling methods. *Food Technol.* **1986**, *40* (6), 55−65.

(32) Favati, F.; Fiorentini, R.; De Vitis, V. Supercritical fluid extraction of sunflower oil: extraction dynamics and process optimisation. *Proceedings of the 3rd International Symposium on Supercritical Fluids*, 1994; pp 305−309.

(33) Zhang, Y.; Yang, J.; Yu, Y.-X. Dielectric constant and density dependence of the structure of supercritical carbon dioxide using a new modified empirical potential model: a Monte Carlo simulation study. *J. Phys. Chem. B* **2005**, *109*, 13375−13382.

(34) Michels, A.; Kleerekoper, L. Measurements on the dielectric constant of CO2 at 25°, 50° and 100° C up to 1700 atmospheres. *Physica* **1939**, *6*, 586−590.

(35) Teuling, E.; Wierenga, P. A.; Agboola, J. O.; Gruppen, H.; Schrama, J. W. Cell wall disruption increases bioavailability of

Nannochloropsis gaditana nutrients for juvenile Nile tilapia (Oreochromis niloticus). *Aquaculture* **2019**, *499*, 269−282.
(36) Jafari, A.; Esmaeilzadeh, F.; Mowla, D.; Sadatshojaei, E.; Heidari, S.; Wood, D. A. New insights to direct conversion of wet microalgae impregnated with ethanol to biodiesel exploiting extraction with supercritical carbon dioxide. *Fuel* **2021**, *285*, 119199.
(37) Patil, P. D.; Dandamudi, K. P. R.; Wang, J.; Deng, Q.; Deng, S. Extraction of bio-oils from algae with supercritical carbon dioxide and co-solvents. *J. Supercrit. Fluids* **2018**, *135*, 60−68.
(38) Weber, N.; Weitkamp, P.; Mukherjee, K. D. Fatty acid steryl, stanyl, and steroid esters by esterification and transesterification in vacuo using Candida rugosa lipase as catalyst. *J. Agric. Food Chem.* **2001**, *49*, 67−71.
(39) van Kuijk, F. J. G. M.; Thomas, D. W.; Stephens, R. J.; Dratz, E. A. Gas chromatography—mass spectrometry method for determination of phospholipid peroxides; I. Transesterification to form methyl esters. *J. Free Radic. Biol. Med.* **1985**, *1*, 215−225.
(40) Geranmayeh, A.; Mowla, A.; Rajaei, H.; Esmaeilzadeh, F.; Kaljahi, J. F. Extraction of hydrocarbons from the contaminated soil of Pazanan II production unit by supercritical carbon dioxide. *J. Supercrit. Fluids* **2012**, *72*, 298−304.
(41) Montgomery, D. C., *Design and Analysis of Experiments*; John Wiley & Sons, 2017.
(42) Esmaielzadeh, F.; Izady, M. M.; Moazzen, J. H. A new experimental correlation using a curve-shaped capacitance sensor to predict liquid holdup in vertical gas-condensate pipelines. *Chem. Eng. Commun.* **2007**, *194*, 495−506.

https://doi.org/10.1021/acsomega.1c04029
ACS Omega 2022, 7, 23027−23040